Energy Reports 7 (2021) 762–777

Contents lists available at ScienceDirect

Energy Reports

journal homepage: www.elsevier.com/locate/egyr

A demand-response method to balance electric power-grids via HVAC systems using active energy-storage: Simulation and on-site experiment

Qinglong Meng [a,c,*], Yang Li [a], Xiaoxiao Ren [a], Chengyan Xiong [a], Wenqiang Wang [a,b], Jiewei You [a]

[a] School of Civil Engineering, Chang'an University, Xi'an, 710061, China
[b] China Qiyuan Engineering Corporation, Xi'an 710018, China
[c] School of Engineering, Cardiff University, Cardiff, CF24 3AA, United Kingdom

ARTICLE INFO

Article history:
Received 16 September 2020
Received in revised form 6 January 2021
Accepted 26 January 2021
Available online xxxx

Keywords:
HVAC
Demand response
Active energy-storage
Air-source heat pump
Cost reduction

ABSTRACT

With the increasing popularity of renewable energy sources and the globally increasing electricity demand, the task of balancing the intermittent energy supply with varying demand becomes increasingly difficult. Instead of adjusting the supply, improving the demand response (DR) can be a more efficient way to optimize power balance. HVAC (heating, ventilation, and air-conditioning) systems, which operate on the demand side of power-grids, have a huge potential to improve the power balance. To assess their potential in a variable air volume (VAV) air-conditioning system with energy storage tank we introduce a demand response method that combines active cool-energy storage (ACES) with global temperature adjustment (GTA). To confirm the effectiveness of this combined ACES+GTA approach, we conduct measurements with the help of a full-scale VAV air-conditioning test setup. The experimental results are compared with a TRNSYS simulation. The measurements indicate that an energy-storing water-tank can effectively reduce the number of starts and stops for the heat pump. The simulation confirms that the ACES+GTA method can also effectively reduce the peak load of the power grid with little impact on the thermal comfort of the energy consumers. The cost-saving rate, compared to the conventional operating mode (no energy-storage during other periods), reaches 7.02% for an entire cooling season if the GTA method (with DR) is used.

1. Introduction

Driven by increasing electricity demand, the global proportion of renewable-energy generation continues to increase (Li et al., 2016). Unfortunately, the intermittent nature and uncertainty of renewable energy sources aggravate the problem of balancing supply and demand within a power grid. In addition, when renewable energy sources are used, the difference between peaks and valleys increased too (Dong et al., 2016). In other words, the power system tends to be poorly regulated and a better regulation method is urgently needed. The relatively new approach, known as demand response (DR), is a promising method to address this problem for conventional power-grids. Demand response, more specifically, is a term that implies that end-users can adjust electricity-demand according to predetermined time-dependent electricity price schemes (e.g. peak- and off-peak-rates). The different tariffs can act as a powerful incentive for electricity consumers to reduce their consumption during peak hours, which reduces peak loads and eases the pressure on stressed power grids (Wang et al., 2010; Yang, 2017).

Buildings, in particular, are typically the main consumers of urban electricity. Fortunately, they also have an enormous potential to benefit from (and contribute to) better peak regulation — especially when using renewable energy sources (Moura and de Almeida, 2010). In addition, the emerging smart grid and Internet of Things provide a suitable hardware platform to introduce a B2G (building to grid) peak-regulation mode. The convertibility between possible multiple energy-sources in a building and the energy-storage ability and characteristics of the building itself make buildings great candidates to implement DR and benefit from it. In commercial buildings, the energy consumption of their HVAC systems accounts for about 40%–60% (Chua et al., 2013). In other words, they are the main consumers of energy. In summer, the HVAC's electric load in commercial buildings accounts for about 30%–50% of a typical city's total peak-load (Lam et al.,

* Corresponding author at: School of Civil Engineering, Chang'an University, Xi'an, 710061, China.
E-mail address: mengqinglong@chd.edu.cn (Q. Meng).
URL: http://js.chd.edu.cn/jzgcxy/mql/list.htm (Q. Meng).

https://doi.org/10.1016/j.egyr.2021.01.083

Nomenclature

c_p	Specific heat (kJ/(kg °C))
F_{save}	Operating-cost savings from active energy-storage systems ($)
$\dot{M}$	Chilled-water mass flow (kg/s)
P	Power (kW)
P_{shed}	Reduction of power (kW)
P_t	Recovery period of the investment (year)
$Q_{i.out}$	Amount of heat exchange between outer building envelope, air infiltration, and indoor air (W)
$Q_{i.in}$	Amount of heat exchange between occupancy, lighting, equipment, furnishings, and indoor air (W)
Q_{AC}	Cooling capacity provided by the variable air volume (VAV) box system to the room (W)
Q_{OA}	Fresh-air load (W)
$RMSE$	Root-mean-square error (−)
ΔT_{ASHP}	Temperature difference between supply- and return-water of air-source heat pump (°C)
ΔT_{AHU}	Temperature difference between supply- and return-water of the air-handling unit (°C)
T	Temperature (°C)
t	Time (h)
V	Volume (m^3)
v	Chilled-water volume flow (m^3/h)
W	Electricity consumption (kWh)

Superscript and Subscript

d.NOR	Daily routine operation method
d.DR	Daily DR operation method
h.NOR	Response-period routine operation method
h.DR	Response-period DR operation method
H	Upper bound
In	Inlet
L	Lower bound
Out	Export
R	Released energy
Set	Set value
S	Energy storage
Tank	Thermal storage tank

Abbreviations

ACES	Active cool energy storage
AHU	Air handling unit
ASHP	Air-source heat pump
CPP	Critical peak pricing
DR	Demand respond
GTA	Global temperature adjustment
HVAC	Heating, ventilation, and air-conditioning
TOU	Time-of-use pricing
RTP	Real-time pricing
VAV	Variable air volume

2010). Hence, the HVAC system can have a large impact on the management of multiple energy sources and their usage on the consumer side, especially when they run in e.g. a B2G peak saving mode. In other words, they can provide a valuable peak-regulation service to the power grid. For instance, on July 30, 2019, the Jiangsu power-grid used an air-conditioning DR-system, which was based on the ubiquitous power of the internet of things, to implement a "peak clipping" DR between 14:00 and 15:00. The HVAC system successfully reduced the load in the grid by 4.02 million kW (Shen et al., 2019).

The exact implementation method is the key for HVAC systems that allows them to participate in the peak-regulation of DR. There are several types of HVAC DR methods — they include simple schedule-switch control (Lee et al., 2008; Yao et al., 2005), duty-cycling control (Xiao-Jin et al., 2006; Xin and Liang, 2013), global-temperature adjustment (Candanedo et al., 2015; Yin et al., 2016), regulation of each unit of the HVAC system. Motegi et al. (2007) and Han and Piette (2007) classified HVAC DR methods for all commercial building types (e.g. offices, supermarkets, libraries) in California. Through actual measurements and simulations, they evaluated the applicability, response effect, and the problems that should be paid attention to in practical applications for 13 different DR methods. These methods include global-temperature adjustment (GTA), duct static pressure (DSP), and cool thermal energy storage (CTES). At present, most of the studies use simulations to verify HVAC DR methods (Amin et al., 2020; Gupta et al., 2018; Hao et al., 2017; Liao et al., 2012; Ran et al., 2020; Wang et al., 2016), and researchers (Beil et al., 2015) performed experiments with DR schemes. Among the many HVAC DR methods, GTA is one of the most mature technologies. For these reasons, GTA was the first verified method in actual engineering scenarios (Xu, 2009), and it was regarded as the most effective HVAC DR method (Piette et al., 2004, 2005).

Furthermore, Zhang et al. (2016) and Yun et al. (2017) analyzed the DR for an American commercial HVAC system and showed that GTA can, in fact, enable commercial construction-operators to adjust the temperature in all components. However, GTA, a commonly used DR method, usually gives little priority to the end-user's comfort. During the implementation of the GTA, the increase for the temperature set point may have a negative impact on the occupants of the building with respect to thermal comfort (Aghniaey and Lawrence, 2018). In addition, conventional DR may cause an increase in total energy-consumption. For example, Beil et al. (2016) conducted a rapid air-conditioning DR for an office building with an area of about 30 000 m^2 and a time interval of 15 min. It was found that the total energy-consumption needed to implement DR was greater for optimized buildings than without DR. Furthermore, Pombeiro et al. (2017) used an air-conditioned room to conduct a comparative experimental study of HVAC DR schemes, based on both genetic algorithms and dynamic programming. The study considered both photovoltaic (PV) power generation and battery storage.

Typical active energy-storage HVAC systems are ice storage and chilled-water storage systems. Unlike ice storage and chilled-water storage systems, which feature large energy-storage capacities but also high initial investment, the active energy-storage systems used for DR can be small-scale. For the case that cool storage air-conditioning systems are part of the DR, Rusa (2015) introduced an evaluation index for cool storage air-conditioning with respect to two "dimensions": energy efficiency and economy. The results show that the cool storage rate of a cool storage

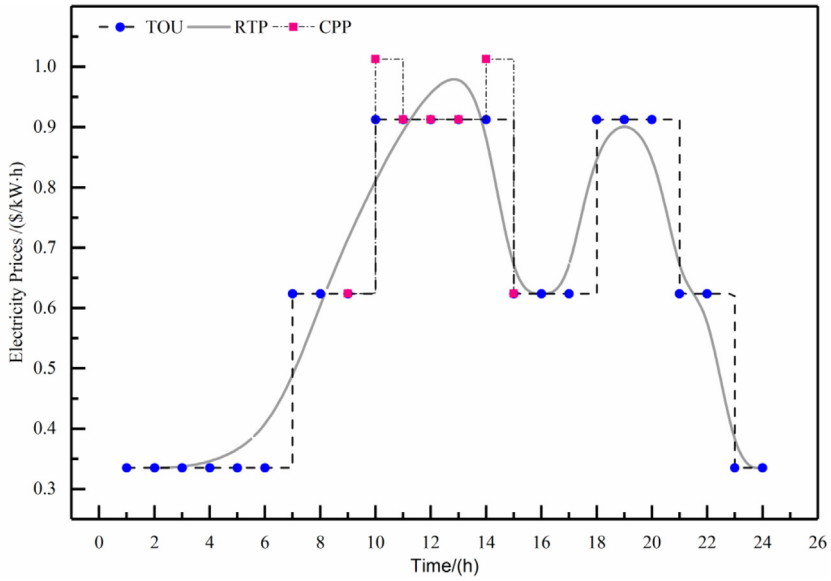

Fig. 1. Three price curves: time-of-use pricing (TOU), real-time pricing (RTP), and critical-peak pricing (CPP).

system, using a peak-through electricity-price system, should not exceed 45%. Dongwen et al. (2017) analyzed the economics of the cool storage air-conditioning system for an actual case. He determined that the optimal cold storage capacity, in this case, was a cold-storage capacity that could meet the demand of 75% of the load on the target day during a local peak-through electricity-price period. The research results show that, when the cool storage capacity was below the optimal cold storage capacity, the total operating cost of the system decreased with increasing cooling needs, and the growth rate decreased gradually. Lo et al. (2016) introduced a DR scheduling model for an ice storage system. The group carried out a simulation study based on a dynamic electricity-price model. The results show that a reasonable scheduling scheme can enable significant energy savings for a cool storage system and improve its operating efficiency and economics. Cui et al. (2015, 2017) simulated DR for an active energy-storage variation that uses phase-change materials. The results show that this approach can decrease the power consumption of the system to 28.9% of the normal power-consumption in a short time and reduce costs. Moreover, to enhance the response potential for building demand, Yan et al. (2015) proposed a chilled-water storage-system (CWS) and a temperature- and humidity-independent control (THIC) air-conditioning system with load-transfer capability to balance real-time power demand. The group used the software EnergyPlus to simulate the system. The results indicate that, compared with conventional air-conditioning systems, the CWS+THIC system improved both the flexibility of a building's energy consumption and its power-load coefficient. Total energy cost could be reduced by 29.7%. Compared with conventional chilled-water storage air-conditioning, the CWS+THIC system can save 64.3% of cold storage volume. In addition to studying active cool storage, Patteeuw et al. (2015) analyzed the potential of active thermal storage systems, which are driven by air-source heat-pumps as part of DR. Furthermore, Jones and Carter (2017) focused on the potential of using distributed energy for DR. The group used a PV system and an energy-storage battery to drive an air-source heat-pump or fan during the DR period, and they simulated the energy-storage method considering thermal comfort.

The above research provides helpful information for both the improvement of DR programs and the construction of an experimental test setup. However, their main focus was ice storage and chilled-water storage, and these studies did not consider the combination of small-scale chilled-water storage-systems and GTA. The present study focuses on small-scale chilled-water storage methods in combination with DR, and we propose a novel DR method (ACES+GTA) that combines GTA with active cool energy storage (ACES). This approach should make it possible to make a building's energy consumption more flexible and improve the ability to control the peak. Unlike previous studies, we utilized the flexibility of small-scale chilled-water storage-system for different cooling-loads. Furthermore, we either included small-scale chilled-water storage-components as part of the DR, or we reduced the frequency of startups and shutdowns of the air-source heat pump (ASHP). Alternatively, we also reduced the operation cost of the system, using different electricity prices. In addition, we introduced the ACES+GTA DR method and analyzed, quantitatively, both conventional GTA and the ACES+GTA method.

The rest of the paper is organized as follows: In Section 2, we created different electricity-price schemes and introduced two DR methods, GTA and ACES. We then introduced both comfort- and economic-evaluation indicators. In Section 3, we conducted the actual measurement using a full-scale experimental setup. The experiments were carried out to assess the feasibility of the proposed method and related operation modes. We also created and ran a simulation, based on TRNSYS, and we quantitatively analyzed the response effects for both GTA and the ACES+GTA method via simulations. The paper ends with conclusions and an outlook for future studies in Section 4.

2. Methodology

2.1. Electricity-price scheme

The premise for the implementation of DR for an air-conditioning system is a good understanding of a suitable electricity-price scheme. Traditionally, there were three different pricing-schemes in the electricity market when price-based programs are used for DR. These are time-of-use pricing (TOU), real-time pricing (RTP), and critical-peak pricing (CPP). To analyze the differences between operation costs for different price-based operation modes, three daily electricity-price curves were used in this paper — see Fig. 1.

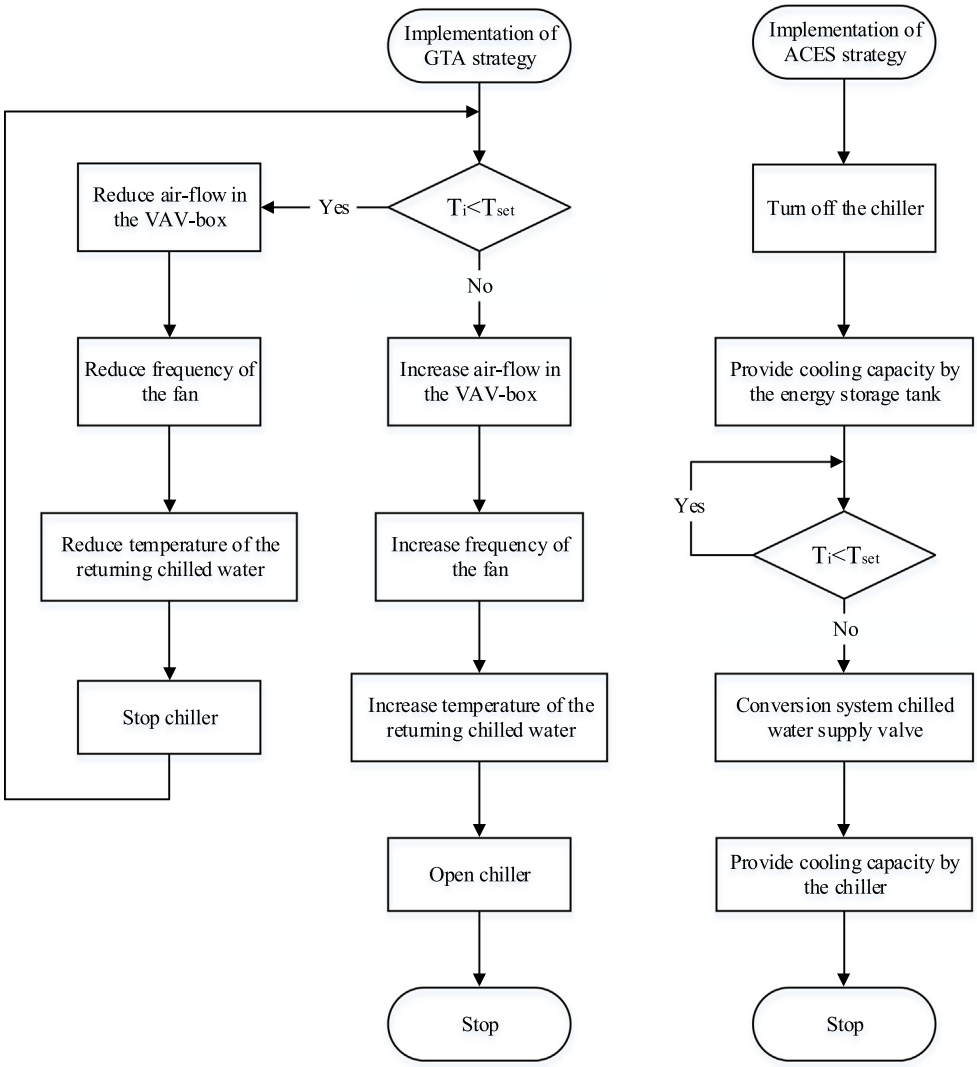

Fig. 2. Schematic of the GTA and ACES DR method.

The TOU curve reflects the current TOU price for industrial and business users who use below 1kV in the province Shaanxi. Because there is no RTP and CPP mechanism in the province Shanxi, this paper uses a B-spline to fit the data of TOU for the province Shanxi to obtain a real-time electricity-price curve. CPP, here, refers to the established standard of CPP in the province Jiangsu. Specifically, based on the original time-of-use tariff, the peak-hour tariff was increased by 0.1 dollars per kWh. CPP was based mainly on temperature data of weather forecasts. If the daily maximum temperature exceeded 36 °C peak electricity prices were applied for 10:00 to 11:00 AM and 14:00 to 15:00.

2.2. DR with GTA- and ACES-method

The GTA method involves controlling the indoor temperature, i.e., setting the temperature value for the terminal room to reduce the demand for cooling or heating during the specified DR period. It also includes the reduction of both the power consumption for the whole HVAC system and the electricity demand of the power grid. When GTA was used to reduce the electric load of the air-conditioning system for large air-conditioning loads in summer, the thermal comfort of users may be decreased due to higher indoor temperatures. Furthermore, the load reduction and response time of the GTA method changes due to variation in a building's thermal inertia. To overcome these limitations of the GTA method and improve the response of the air-conditioning system DR, a DR method that can take into account active energy-storage was proposed in this paper.

The GTA and ACES methods are two methods that operate independently. The DR flow for the GTA- and the ACES-methods is shown in Fig. 2. The two methods enable load reduction of the HVAC system at the indoor end and at the cold source, respectively. According to Fig. 2, following the implementation of the GTA method, and due to the thermal inertia of the building, the actual indoor air-temperature changes only slowly. Before reaching the new set indoor-temperature, for the variable air-volume system (VAV) air-conditioning system, the VAV-box reduces both the air supply to the room and the frequency of fan usage. In addition, the return temperature for chilled-water to the ASHP was turned off. When the actual air-temperature reaches the set-point temperature, the air volume of the VAV-box increases, and the fan frequency and the chilled-water return temperature were increased until the ASHP restarts. The ACES method was implemented by a control system that shuts down the cooler and switches the valve. In addition, the active cold-storage component provides the required cooling capacity for the air-conditioning terminal. When the energy-storage device cannot supply the required cooling-capacity at the current room set-point temperature, the indoor temperature in the air-conditioned

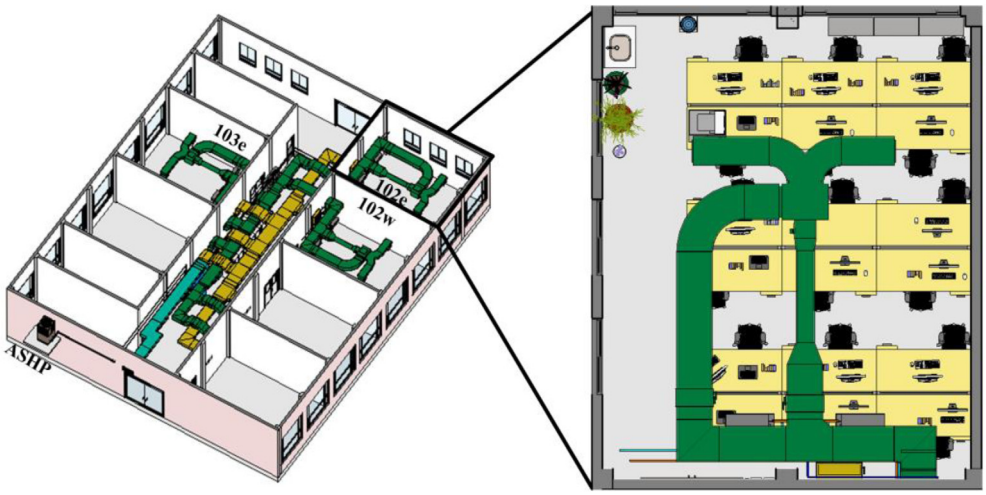

Fig. 3. Three-dimensional schematic of the test setup.

Table 1
Grading of the effect of indoor temperature change on thermal comfort.

Temperature interval (°C)	[26,26.5]	[26.5,27]	[27,27.5]	[27.5,28+]
Impact level	0	1	2	3

room would increase. When the actual temperature exceeds the set-point temperature, the chiller activates and enables cooling. The chiller used in this article is an air-source heat-pump (ASHP). Furthermore, we compared the effect of independent operation with joint operation for the GTA and ACES methods in the experiment. We analyzed, in detail, the effect of the independent application of the GTA method and the combined application (GTA+ACES).

2.3. The evaluation index

Because, an aggregation of loads would be needed on the power-grid side, an accurate analysis would be difficult. For the user side, however, we can use both the comfort index and economic index to evaluate the operation mode.

2.3.1. Thermal-comfort rating

To quantify the effect of temperature change (induced by the DR method) on the thermal comfort, we divided the temperature range 26–28+ °C into four intervals: the impact levels 0, 1, 2, and 3. When the clothing insulation is 0.5Clo, the upper limit temperature of thermal comfort is about 28 °C. This limit temperature is defined by the indoor thermal comfort zone in the ASHRAE Handbook (ASHRAE, 2013). These indicate, respectively, no impact, slight impact, minor impact, and impact — see Table 1. To show the effect of the different DR methods on the thermal comfort of users, and the actual temperature-range in the cooled room (Table 1) was used to define the different assessment grades.

2.3.2. Economic indicators'

(1) Daily operating-cost

For the DR of the air-conditioning system, the main costs are the operating cost and the incentive subsidies from participating in the DR. We refer to the subsidy standard of Shanghai: the annual number of single-user demand side responses does not exceed 10, and the total duration is a maximum of 10 h, while peak cutting and valley filling are subsidized at 0.43 $/kWh and 0.17 $/kWh, respectively. To compare the economics between the different methods, we calculated daily power-saving rates and daily cost-saving rates:

$$\alpha_{\mathrm{d.save}} = \frac{W_{\mathrm{d.NOR}} - W_{\mathrm{d.DR}}}{W_{\mathrm{d.NOR}}} \times 100\% \tag{1}$$

$$\alpha_{\mathrm{DR.save}} = \frac{F_{\mathrm{h.NOR}} - F_{\mathrm{h.DR}}}{F_{\mathrm{h.NOR}}} \times 100\% \tag{2}$$

$$C_{\mathrm{d.run}} = F_{\mathrm{d.DR}} - E_{\mathrm{DR}} \tag{3}$$

Here, $\alpha_{\mathrm{d.save}}$ is the daily power-saving rate of the air-conditioning system, in %. $W_{\mathrm{d.NOR}}$ and $W_{\mathrm{d.DR}}$ were the daily power-consumption of the air-conditioning system for conventional operation and DR, respectively, in kWh. Furthermore, $\alpha_{\mathrm{DR.save}}$ represents the cost-saving rate for the DR period, in %. $F_{\mathrm{h.NOR}}$ and $F_{\mathrm{h.DR}}$ were the running costs of the regular operation method and the DR method, respectively, during the DR period, in $. $C_{\mathrm{d.run}}$ denotes the daily cost of the air-conditioning system, in $. $F_{\mathrm{d.DR}}$ was the daily operating cost using the DR method, in $. E_{DR} was the incentive subsidy cost, which was obtained by participating during DR, in $.

(2) Total operating-cost

To highlight the economics of active energy-storage, we put forward Equation (4) for the total operating cost of active energy-storage:

$$F_{\mathrm{save}} = (F_{\mathrm{run.DR}} + F_{\mathrm{run.NOR}} + E_{\mathrm{DR}}) - \mathrm{F'}_{\mathrm{run.NOR}} \tag{4}$$

Here, F_{save} was the cost saving of HVAC systems, for active energy-storage, and $F_{\mathrm{run.DR}}$ was the operating cost for the days, when DR was implemented. $F_{\mathrm{run.NOR}}$ was the operating cost for conventional operating days of energy storage. E_{DR} was an additional subsidy for the benefit of the grid, when DR was involved, and $F'_{\mathrm{run.NOR}}$ was the cost of running the system without energy storage.

The operating-cost calculations in this paper were done in US dollars ($). The exchange rate for the USD to RMB was 1:7.

3. Results and discussion

3.1. Experimental

3.1.1. The test setup

The full-scale HVAC-system test setup was located on the first floor of the Xiaozhai campus of Chang'an University. The layout of the laboratory's HVAC system and its terminal rooms is shown in Fig. 3. The three air-conditioned rooms are 102e, 102w, and

(a) Air-source heat pump (b) Air-handling unit

(c) Energy storage tank (d) Room terminals

Fig. 4. Main components of the test setup.

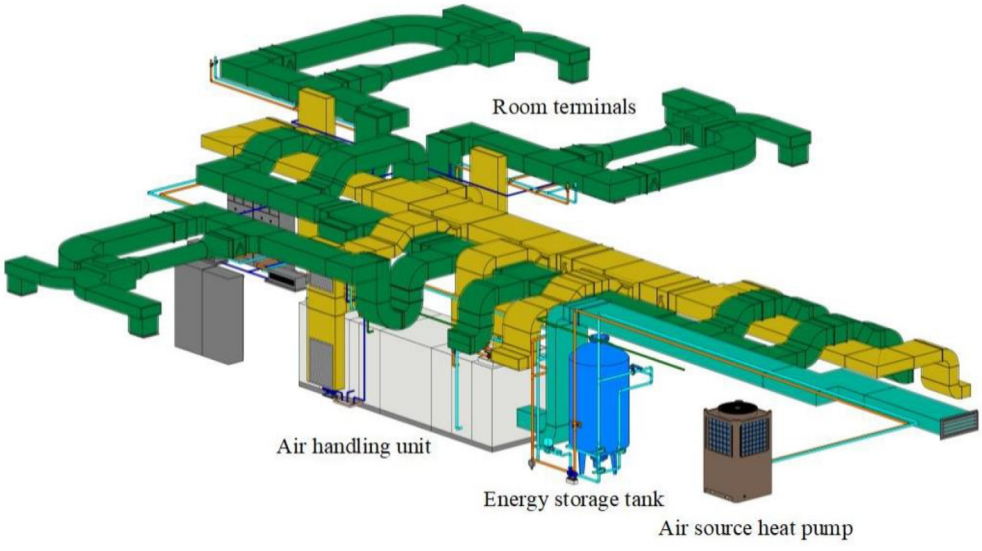

Fig. 5. Three-dimensional diagram of the air-conditioning system.

103e, respectively. The three rooms are 64.8 m^2 (7.2 m × 9 m) in area.

The variable-air-volume system, to take into account active energy-storage, mainly includes an air-source heat-pump, a 2.3 m^3 energy-storage tank, air-handling unit (AHU), air ducts, water pipes, VAV terminals, basic metering-equipment, and a control system. The energy storage tank, AHU, and control cabinet were placed in the corridor, and the ASHP was placed on the platform on the west side of the laboratory. Photos of the main components were shown in Fig. 4. A virtual 3D diagram of the whole

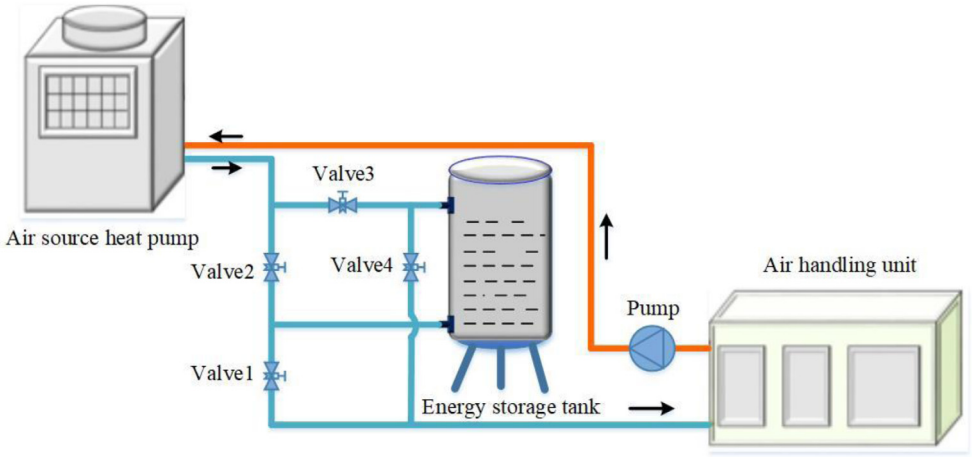

Fig. 6. Schematic of the water-flow system with active energy-storage.

Table 2
Most important parameters of the used components.

Name	Type	Number	Flow/m^3/h	Power/kW
ASHP	MAC100DR-FAB	1	–	9.8
Pump	MHI403-1/10/E	1	8	0.78
AHU	TZK-05Z	1	5000	2.2
VAV-box	RSV-TU-1-I-07-L	3	208–1800	–

air-conditioning system is shown in Fig. 5. The performance parameters of the biggest power-consuming components are shown in Table 2.

The energy-storage tank in the test setup is a key component. The volume of the water tank is mainly determined by the air-conditioning load, the released-energy time of the energy-storage tank, the difference between the average maximum-temperature of the energy-storage tank at the beginning of storing period and the average minimum-temperature of the energy-storage tank at the end of the storing period. The larger the volume of the water tank is, the larger is the stored energy. While this makes it possible to better benefit from lower electricity prices, it often leads to greater investment costs too. The control system can control (remotely) all HVAC components, e.g., ASHP, fan, pump, and valves through the host computer. The host computer receives the parameters of both the water system and wind system via the sensors located in the water pipes, air ducts, and the energy storage tank. These parameters include the supply- and return-water temperatures for the chilled water, the air-supply temperature, and the water temperature of the energy-storage tank. The main goal of this experiment was to study the application of active energy-storage with different DR operation methods. Hence, the energy-storage tank was the key component. It was equipped with two upper and lower cold/hot-water inlets/outlets. The four electromagnetic valves, which were attached to the inlet and outlet pipes (shown in Fig. 6), could be used to switch between winter and summer operating modes. In addition, switching between hot- and cold-water flow through the energy storage water tank could also be achieved by solenoid valves. The switching status of the ASHP and solenoid valves, and the direction of the water flow in the energy-storage tank for the different operating modes, are listed in Table 3.

3.1.2. Measurement principle

In summer, the air-conditioning cooling-load peak of buildings generally occurs between 14:00 and 16:00, which was also the peak of the power load of the grid. Therefore, this study assumes that DR events occur between 14:00 and 16:00. For the experiment, we selected a week of continuous high-temperature weather in Xi'an from August 14th to August 20th. To take into account both the energy storage and no energy-storage operation modes, different DR methods, and different operation periods, we selected six operation methods (see Table 4) to compare: ST1, ST2, and ST5 were the daily operation methods without DR, ST3, ST4, while ST6 was the daily operation method with DR. The indoor temperature setting for ST3 and ST6 (to implement GTA) was 28 °C for the DR period (14:00–16:00). All other methods set the room temperature to 26 °C for the entire HVAC system operation. During the test, ST1 and ST2 were used to compare and analyze the effect of active energy-storage components on the whole system, ST2 and ST5 were used to study the effect of different energy storage and energy release periods on the conventional operation of active energy-storage, ST3, ST4. ST6 was used to compare the effect of the response of GTA, ACES, and ACES + GTA on the DR methods.

3.1.3. Results and analysis

The time-averaged power of the six methods (ST1, ST2, ST3, ST4, ST5, ST6) and the changes with outdoor air-temperature (during the corresponding hours) are shown in Fig. 7. The lines in Fig. 7 are due to the B-spline interpolation of the time averaging power associated with different operating methods. Although the time-averaged outdoor air-temperatures of the six methods were different at different times, the temperature trends were identical. At 14:00–16:00 of a day, the outdoor air-temperature reached a peak, which was also the peak of the building's cooling load and the electricity consumption of the air-conditioning system.

By analyzing six kinds of time-averaged power changes, we could perform a comparative analysis of the different methods. Compared to ST1, ST2 needed to store energy for the energy-storage tank and cool the room after 9:00, and the operating power of the system was relatively large. Compared with ST1, ST3 increased the room-temperature setting by 2 °C from 14:00 to 16:00, and the power load of the system was reduced during the DR period. On hot days, although the target room temperature was increased, the indoor cooling-load was still relatively high, and the true reduction of the electricity load was limited. The ST4 method provided the required cooling capacity to the AHU with the help of an energy-storage tank and a shut down of the ASHP during the DR period. The reduction in electricity load for ST4 was improved significantly compared to ST3. After analyzing the operating modes ST4 and ST6, it can be concluded that the outdoor air-temperature for ST6 was higher than that for ST4, and the power consumption for ST6 during actual operation was also significantly higher.

Table 3
Switch status for the ASHP and solenoid valve for the different operating modes.

Operating conditions	ASHP	Valve 1	Valve 2	Valve 3	Valve 4	Water-flow direction of storage tank
Summer energy-storage	On	Off	On	Off	On	Bottom-in top-out
Summer energy-release	Off	On	Off	On	Off	Bottom-out top-in
Non energy-storage	On	On	On	Off	Off	–

Table 4
Operating modes for the six methods.

Methods	Operating mode	Operational period	Energy storage period	Energy release period
ST1	Conventional (no) energy-storage	9:00–18:00	–	–
ST2	Conventional energy-storage	9:00–18:00	9:00–10:00	17:00–18:00
ST3	GTA	9:00–18:00	–	–
ST4	ACES	8:00–18:00	8:00–9:00	14:00–16:00
ST5	Improved conventional energy-storage	8:00–18:00	8:00–9:00	16:00–18:00
ST6	ACES+GTA	8:00–18:00	8:00–9:00	14:00–16:00

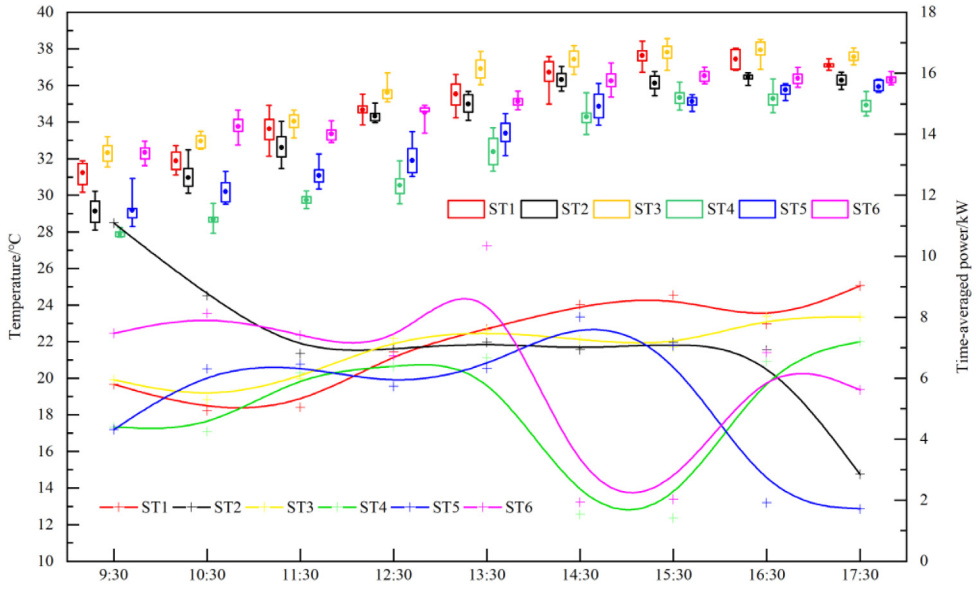

Fig. 7. Time-averaged power for the six methods, and the changes of outdoor temperature during the measured hours.

The average outdoor air-temperature and the power consumption for each unit of the air-conditioning system, during the operation using the six operating methods, are shown in Fig. 8. The figure shows that the ASHP accounts for most of the energy consumption of the air-conditioning system for all methods. The next highest energy consumers are the fan and the pump. For the different daily operation-methods, the changes in the electricity consumption of the ASHP are most significant. This is followed by the fans, while the water-circulation pumps showed the lowest consumption.

Even though the average outdoor air-temperature for ST1 was slightly higher than for ST2, the system power consumption for ST1 was lower than for ST2. This difference in power consumption indicates that the conventional operating-method, which considers active energy-storage, could increase the power consumption of the air-conditioning system.

The average outdoor air-temperature of SST1 was lower than for ST3, and the power consumption of the system was higher than for ST3. This shows that the GTA method could successfully reduce the power consumption of the system.

A comparison between ST2 and ST5 shows that the improved active energy-storage conventional operation modes can effectively reduce the power consumption of the ASHP. After comparing ST4 and ST6, it was found that the ACES+GTA operating modes increased the power consumption significantly. There are two main reasons for this: The first reason is that ST6 performs energy storage at 8:00–9:00,when the outdoor air-temperature was higher than ST4's. This led to an increase in the power consumption of the ASHP during the energy-storage period. The second reason is that the average outdoor temperature, during the days when ST6 was implemented, was significantly higher than for ST4. This increases the cooling load and the power consumption of the air-conditioning system on the day when ST6 was used.

Thanks to the experimental data, we could also determine the temperature changes for the supply- and return-water of the ASHP and AHU, with no energy storage and the energy storage conditions — see Fig. 9(a) and (b). Compared with ST1, ST5 with the ASHP and AHU, the frequency of fluctuation of the inlet and outlet water temperature curve was reduced significantly. In addition, the amplitude of the fluctuation was reduced. The number of switches of the ASHP decreased from 43 to 7. In the experiment, the on–off control mode of the ASHP was the following: When the inlet temperature of the ASHP exceeded 13 °C, the compressor began to operate. When the inlet temperature of the ASHP fell below 10 °C, the compressor was switched off. Therefore, only when the inlet temperature of the ASHP was between 10 °C and 13 °C, the compressor could run stably, without the risk of being controlled. Then, the indoor cooling-load was below the cooling load with ST1 method, and the air-conditioning system was in the "high flow, low load" operating mode. This ensured that the temperature difference between the supply- and

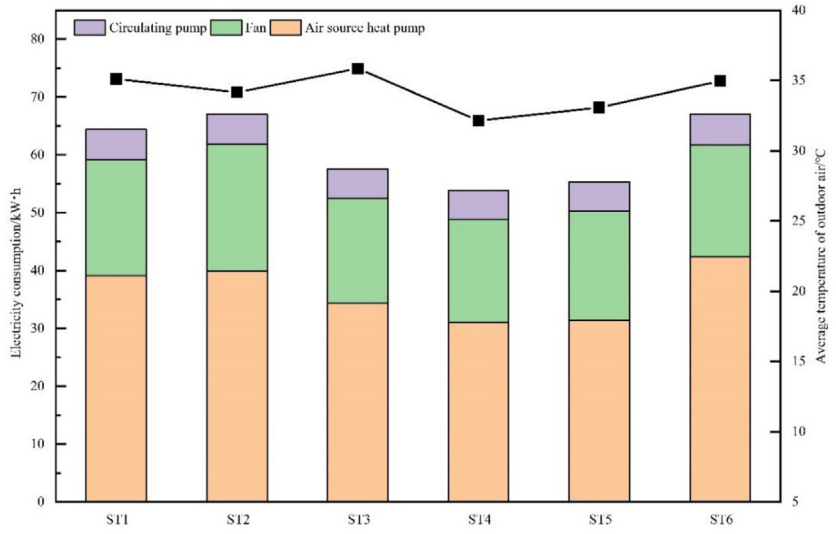

Fig. 8. Power consumption for each unit of the air-conditioning system and average outdoor air-temperature change.

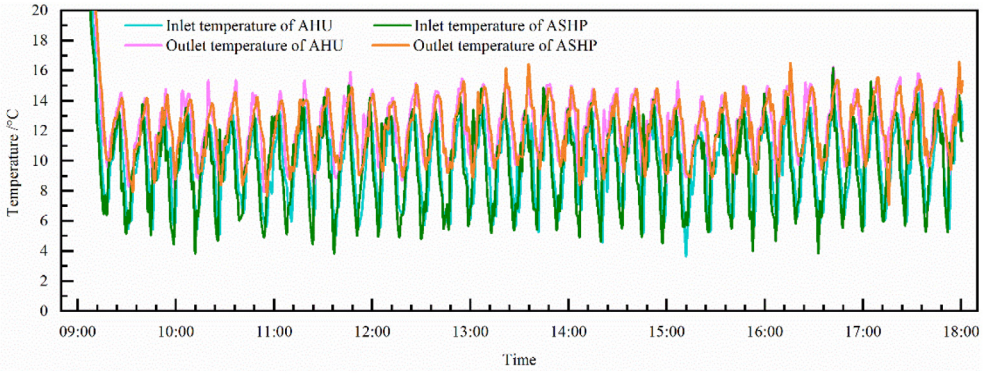

(a) ST1

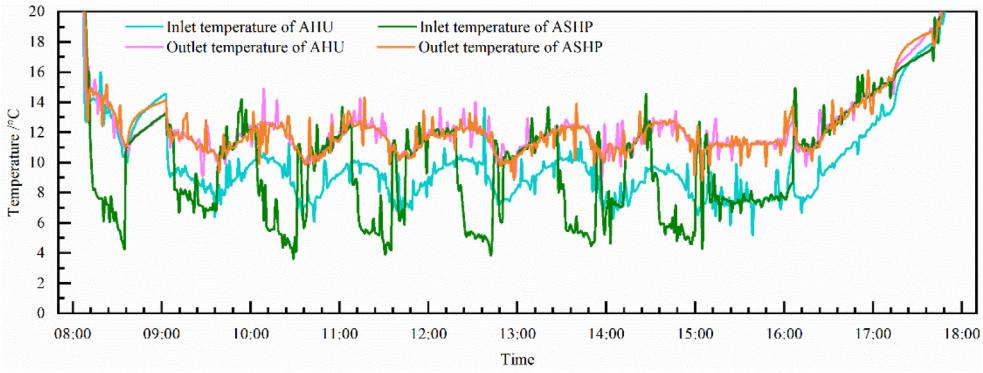

(b) ST5

Fig. 9. Water temperature changes for the different operating methods in summer.

return-water of the AHU was below the ASHP inlet and outlet water-temperature difference. As a result, the ASHP underwent frequent starts and stops — see Fig. 9(a). For the ST1 method, the changes in the inlet and outlet water temperature of ASHP and AHU tended to be consistent. The starts and stops of the compressor directly affect the change of the inlet water temperature of the AHU, and the value of the inlet water temperature of the AHU determined the start and stop of the compressor. When the temperature difference between supply- and return-water of the AHU was small, this increased the number of starts and stops for the compressor. With the ST5 method, the water-temperature difference between the inlet and outlet of the energy-storage tank served as an important buffer — see Fig. 9(b). When the compressor was active, due to the water temperature of the energy storage, the inlet water-temperature of the AHU was not immediately affected by the outlet temperature of the ASHP. This effectively reduces both the water-temperature changes of the

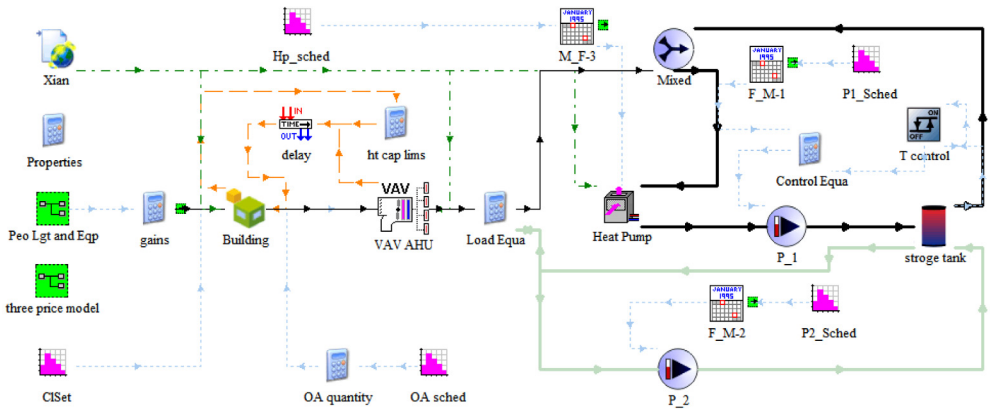

Fig. 10. Schematic of the HVAC DR simulation that takes into account active energy-storage.

Table 5
Explanation of the most important simulation modules.

Icon	Module	Function
	Type56	Establish a three-dimensional building energy model to obtain the specific values of different parameters for the building's cooling and heating load and indoor air as a function of time
	Type151	Treat the air, which flows to the air supply point, and send it to the end of the room and adjust the air volume through the variable air volume (VAV) terminal
	Type0	Calculate the building cooling and heating load, created by personnel, equipment, and light, and edit the relationship between the building cooling and heating load and the flow of chilled water. In addition, output the return water temperature and flow of chilled water
	Type2	Switch of the chilled-water pump, which is controlled by the temperature difference between inlet and outlet of the energy-storage tank
	Type14	Use linear interpolation to generate discrete data for a continuous function of force within a day, which is a control signal for the operating state of the equipment
	Type150	Delayed output of the latent-heat release rate, which simulates the building's thermal inertia and optimizes the building model

outlet temperature of the ASHP and the inlet temperature of the AHU — in addition to the number of switches of the ASHP.

3.2. Simulation

The experiment tested the feasibility of the ACES method using a full-scale test setup. In these experiments, each operating method had different meteorological outdoor parameters: building heat, lighting, and equipment. Hence, it was not possible to quantitatively analyze the effect of the different DR methods on the operation of the air-conditioning system if active energy-storage was to be considered. Even if the same DR methods had been used in the experiment, due to limiting objective factors, the actual operation results would have been very different. Therefore, we created a TRNSYS simulation to conduct a further analysis of the outcome for the experiment. Unlike the study and analysis of the feasibility of the operating mode in the experiment, the simulation focused on a quantitative comparison and analysis of the operation effect of the GTA and ACES+GTA for different conditions. In addition, we performed an in-depth study of the economics of the energy storage system for three different electricity-pricing schemes.

3.2.1. Details of the simulation model

We used TRNSYS software to create a transient simulation-system, with the experimental test setup as the simulation object, see Fig. 10. The main simulation modules, which are shown in the figure, are shown in Table 5.

The TRNSYS simulation platform was built, starting from the air-conditioning system and ending with the cold source. The indoor heating-parameters (personnel, equipment, lighting) and room temperature at the end of the room were first entered into the TRN3D multi-region building-model Type56. The operation data for fresh-air volume and the cooling load of the terminal room were input into Type151 (VAV+AHU). The latter is a combination of the room VAV terminals and the AHU, which is used to obtain the cooling load for the entire air-conditioning system. Furthermore, we edited the load equation in the calculator Type0 to solve the water system that required cold water flow, and we modeled the circulation of the chilled-water system. In Fig. 10, the chilled water passes through the P1 water-circulation pump during the "no energy release" period, while the chilled water passes through the P2 water-circulation pump during the energy-release period. The temperature control of the energy storage water tank in the figure was achieved using an on–off controller (Type2) and the time-forcing function Type14. An output delay (Type150) was used to simulate the effect of the building's thermal inertia on the room's instantaneous cooling load. Finally, using three types of electricity price models, and the power consumption of each component of the air-conditioning system, the cost equation was established in Type 0 to output the operating cost of the air-conditioning system.

To verify the effectiveness of the simulation model (compared to the measured power of the main components of the system in the experiment ST1), we analyzed the simulated values, which were obtained by the simulation, using the conventional method. The power change for the ASHP is shown in Fig. 11. For the operating condition of two sets of compressors, the measured value of ASHP power agreed with the simulated value. Using Eq. (5) we can show that the two sets of ASHP compressors were operating correctly. The root-mean-square error of the air-source heat-pump power was 0.278 kW.

$$RMSE = \sqrt{\frac{\sum_{i=1}^{n}(P_m - P_e)^2}{n}} \tag{5}$$

A comparison between the measured and simulated power of the fan and the pumps is shown in Fig. 12. The mean of the absolute error of the water pump was below 0.01 kW, and the mean of the absolute error of the fan was below 0.03 kW. In Fig. 12, for 12:30–13:30 and 16:15–16:30, the measured fan

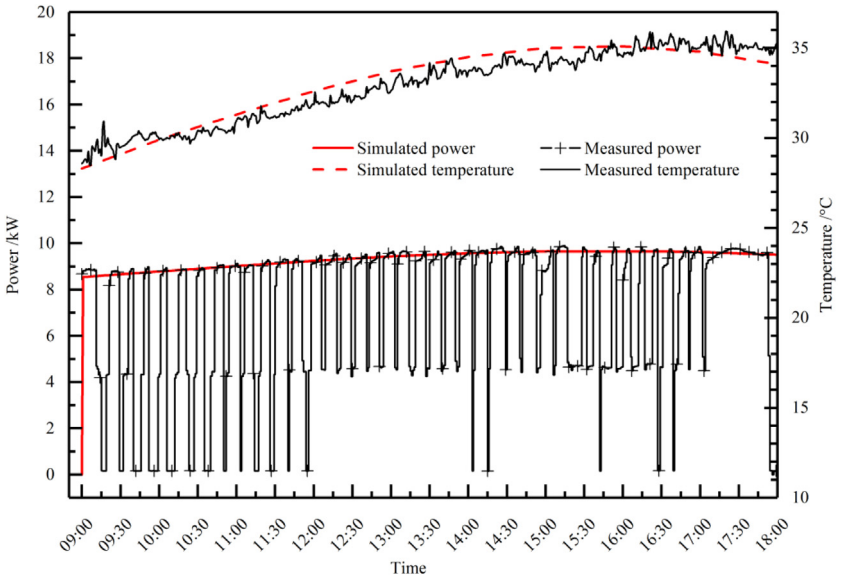

Fig. 11. Measured and simulated power for the air-source heat pump.

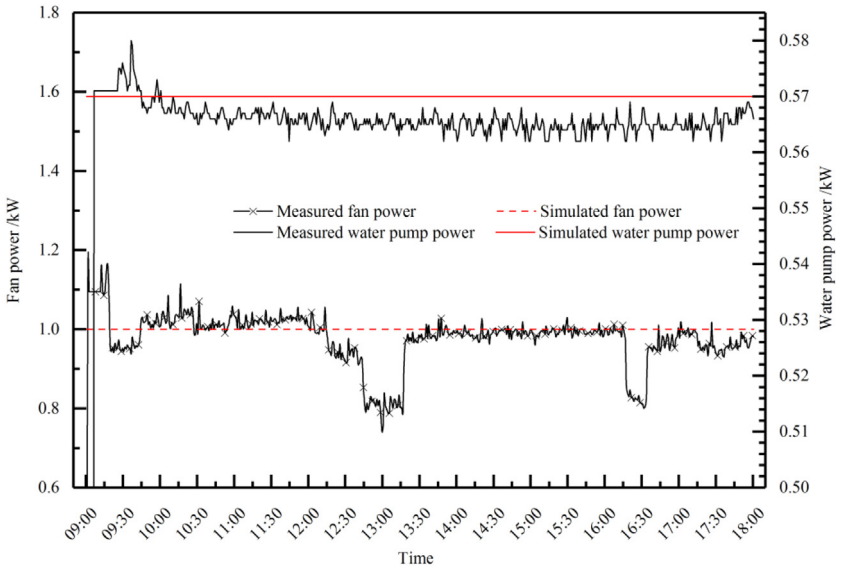

Fig. 12. Measured and simulated power for the fans and pumps.

power decreased significantly. This may be caused by the reduction in required air-flow. The outflow of personnel during lunch breaks (from 12:30 to 13:30) in the office was caused by a reduction of indoor-personnel load. Furthermore, the automatic damper of the VAV-box was adjusted downward, and both the frequency and power of the fan were also be reduced. The change in fan power for the period 16:15-16:30 could have resulted in an outflow of personnel due to objective factors of the day. For example, some indoor personnels were attending a lecture by a coworker, which could have caused the fan power to decrease during this period.

3.2.2. Simulation scheme

The DR of the air-conditioning system to participate in the "peak cut" usually occurred during hot weather in summer. Because hot days generally lead to higher power-consumption, three typical days (in summer) with high power-consumption by the air-conditioning system were selected. The related outdoor air-temperature parameters are shown in Table 6. The average outdoor air-temperature decreased as a result, and the DR simulation, using the GTA and ACES+GTA method, was carried out on three typical days. To simulate the DR with the GTA method, we set the indoor temperature T_{set} to 26 °C, 27 °C, and 28 °C during DR (14:00–16:00 for each day). Moreover, we conducted the simulation for three typical days. For the ACES+GTA method, when active energy-storage was considered, the duration of energy release from the energy-storage tank, using Eq. (6), was t_R of about 0.9 h. To simplify the analysis, we assumed that the active

Table 6
Three typical daily outdoor-temperature changes.

Typical day	All-day T_{out} range (°C)	Yesterday T_{out} range (°C)	DR Times T_{out} mean (°C)
Day1	24.3–36.5	19.2–32.2	36.1
Day2	25.7–36.1	23.2–31.7	35.7
Day3	23.2–35.1	24.3–36.6	34.8

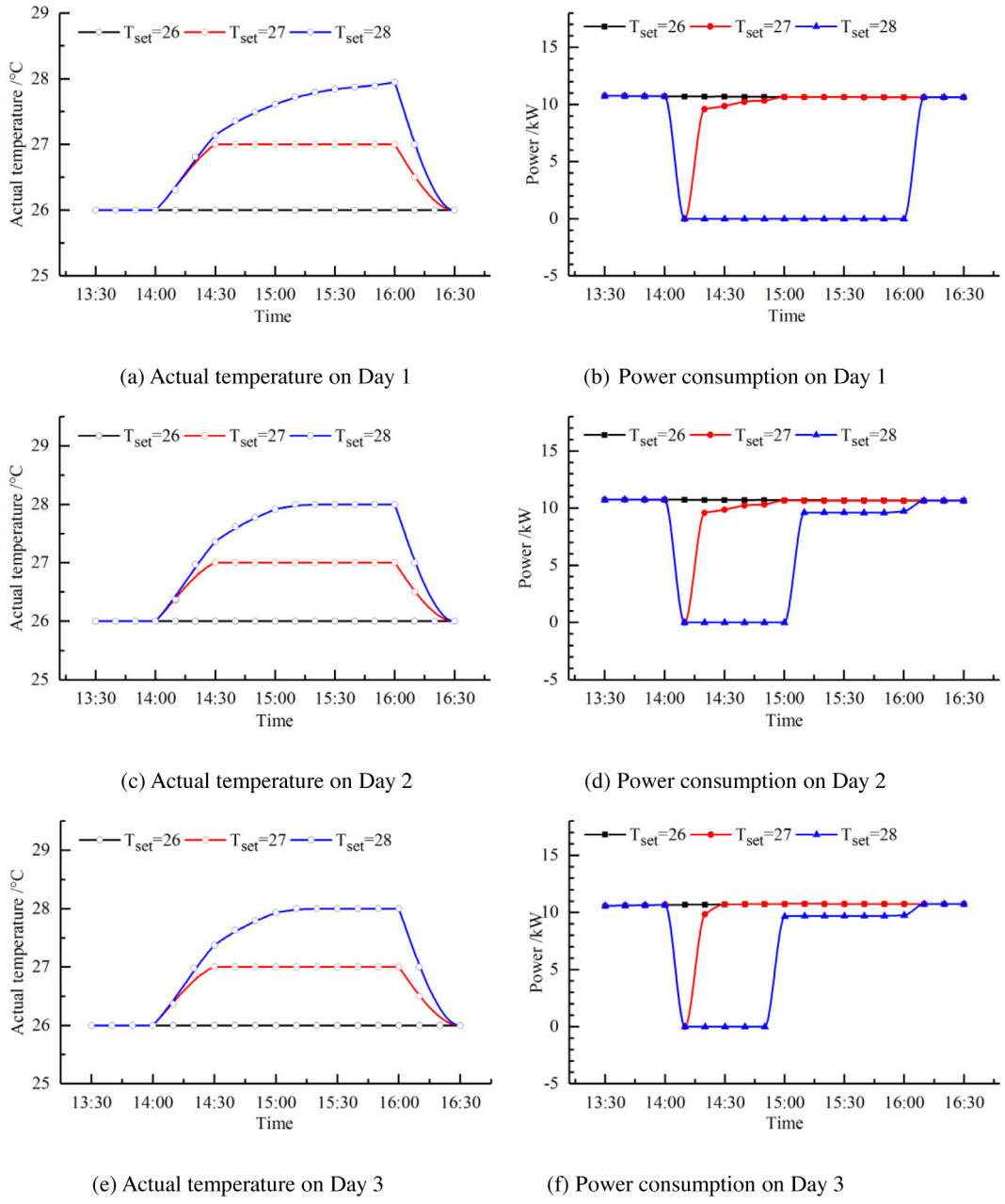

Fig. 13. Actual room temperatures for the GTA method, and the power consumption of the corresponding air-conditioning system.

energy-storage method worked as follows: The ACES method was implemented during 14:00–15:00, which used an energy-storage tank to enable cooling. The GTA method was implemented during 15:00–16:00, and the set point for the indoor temperature was adjusted to 27 °C or 28 °C. To verify the ACES+GTA method, we conducted simulations on three typical days.

$$t_R = (V/v) \times \left(\frac{T_{h.out} - T_{l.out}}{\Delta T_{AHU}} \right) \quad (6)$$

Here, t_R was the energy-release time for the tank. The volume of the energy-storage tank V was 2.3 m^3. The volume flow rate of chilled-water v was 4.6 m^3/h, when releasing energy. $T_{h.out}$ and $T_{l.out}$ were the upper and lower limits for the outlet temperature of frozen water during energy release, which were 1 °C and 7 °C respectively. The temperature difference between supply water and return water for the cold-water coil in the combined air-conditioning unit, ΔT_{AHU}, was 5 °C.

3.2.3. Simulation results

(1) GTA simulation

After simulating the GTA method for three typical days, the actual indoor-temperature changed, and the power consumption of the air-conditioning system (the combined power consumption of fan and ASHP) for different outdoor conditions are shown in Fig. 13. As shown in Fig. 13(a) (b), using a set point of 26 °C as the baseline, there are two scenarios: When the set (target) value, T_{set}, the actual indoor-temperature was changed from 26 °C to 27 °C, the actual indoor temperature reached 27 °C within half an hour — due to thermal inertia of the building. The actual ASHP power-reduction time was below half an hour. When the T_{set} was increased slightly more, from 26 °C to 28 °C, the actual indoor temperature did not reach 28 °C before the end of the DR period, and the reduced system power time was not below 2 h. Fig. 13(c) (d) shows two other scenarios: When T_{set} was adjusted from 26 °C to 27 °C, the indoor actual temperature reached 27

°C in half an hour, and the power-reduction time was below half an hour. However, when T_{set} was adjusted from 26 °C to 28 °C, it took about one hour for the actual indoor temperature to reach 28 °C, and the system power reduction lasted one hour. Fig. 13(e) (f) illustrates another two scenarios: When T_{set} was adjusted from 26 °C to 27 °C, the actual indoor temperature did reach 27 °C in about half an hour, and the power-reduction time was below half an hour. When T_{set} was adjusted from 26 °C to 28 °C, it took below about one hour for the actual indoor temperature to reach 28 °C, and the reduced system power time was below one hour.

By comparing the actual room temperature for three typical days with the power consumption of the air-conditioning system during the DR period, it can be seen that the actual room temperature reached the new target value just after 30 min after increasing the room temperature setting from 26 °C to 27 °C during the DR period. For a fixed set indoor-temperature of 27 °C, the reduction in power consumption for the air-conditioning system was limited. Compared with the set value of 28 °C for the DR period, the response time of the air-conditioning system became shorter. When the room temperature set-point (the target temperature) was increased by 2 °C from 26 °C, for the three typical days, the power consumption reduction and response time of the air-conditioning system increased significantly. In addition, after comparing the response times from Fig. 13(b) (d) (f), when T_{set} was set to 28 °C during the DR period, different typical days showed clearly-different response times.

By comparing the changes of the actual indoor-temperature and power consumption for the air-conditioning system on Day1 and Day2, it was found that, when the building's cooling load was high during the DR period, the time it took the actual indoor temperature to reach the new target room temperature (for the DR period) became shorter. In addition, the DR time decreased and the potential for "peak clipping" became smaller. Due to the thermal inertia of the building, although the average T_{out} during the DR period of Day1 exceeded the average T_{out} of Day2, the hourly cooling load of the building during the DR period was lower than for Day2. Therefore, when the GTA method was used to cut the peak and DR was used, the grid's peak-cutting potential was not stable. Instead, the response time for the peak cut changed due to changes in both the building's cooling load and the outdoor air-temperature on that day.

(2) ACES+GTA simulation

The results for the ACES+GTA method for three typical days are shown in Fig. 14. As shown in Fig. 14(a), using a set point of 26 °C as the baseline, we obtained two scenarios: When the GTA method was implemented, at 3pm on a typical day, the indoor temperature set value, T_{set}, was adjusted from 26 °C to 27 °C, and the actual indoor-temperature reached 27 °C within a quarter of an hour, due to the thermal inertia of the building. When T_{set} was adjusted from 26 °C to 28 °C, the actual indoor-temperature took one hour to reach 28 °C. As shown in Fig. 14(a) (c) (e), the actual indoor-temperature changes for Day2 and Day3 were roughly the same. From Fig. 14(b), we can see that, when the air-conditioning system used the ACES method at 14:00, the power consumption was greatly reduced, and after the GTA method had been implemented at 15:00, the power consumption was reduced further. When T_{set} was 27 °C, the system turned on the cooler after more than fifteen minutes, which caused the system power consumption to increase substantially. When T_{set} was set to 28 °C, the system power consumption remained until the end of the DR period. For Fig. 14(d) (f), when T_{set} for the GTA method was 28 °C, the power consumption changes, using the ACES+GTA method on Day2 and Day3, were the same as for Day 1. This met the reduction requirements. When T_{set} for the GTA method was 27 °C, the power consumption changes, using the ACES+GTA method for different typical days, were the same. However, the power-consumption reduction period for Day1 was slightly longer than for Day2 and Day3. By analyzing the power-consumption curves for different typical days, we can conclude that both the power-consumption reduction and response time, using the ACE+GTA method, were more stable and less affected by the weather.

Table 7
Impact of two DR methods on thermal comfort.

Temperature range	[26,26.5]	[26.5,27]	[27,27.5]	[27.5,28]
Impact level	0	1	2	3
GTA	16.7%	8.3%	8.3%	66.7%
ACES+GTA	55.8%	6.7%	11.7%	25.8%

3.2.4. Comparison of the DR methods

(1) Response times

The simulation results for the GTA method indicate that the DR of the air-conditioning system produces two scenarios due to the thermal inertia of the building. One scenario is that, for a relatively low cooling-load of the building, the air-conditioning system consumes much electricity during the DR period due to the high outdoor air-temperature. The second scenario was that both the cooling load of the building and the outdoor air-temperature were relatively high during the DR period. In the former case, the GTA method could achieve no ASHP response times below 2 h by increasing the target room temperature value. On the other hand, the ACES+GTA method extended the energy discharge time for the energy-storage tank due to the relatively low cooling load of the air conditioner. For the second scenario, using the GTA method to increase the target room temperature, while ensuring that the indoor temperature remains within the acceptable temperature range of the user, the ASHP response-time did not exceed 2 h. On the contrary, the ACES+GTA method takes into account active energy-storage, which increases both the "peak-shaving" potential of the air-conditioning system and the flexibility for energy use. The cooling capacity of the energy-storage tank could be used to meet the grid response time requirements. In addition, regardless of whether the cooling load of the building was high or low, the GTA method, combined with active energy-storage, could meet the 2 hours response-time requirement. Simultaneously, the ACES+GTA method was able to use a larger response-time control range to avoid the adverse effects of a load rebound.

(2) Impact on thermal comfort

Compared with the GTA method, which mainly realizes DR by resetting the indoor temperature, the ACES+GTA method can use the energy store tank to release energy. In this way, it was possible to enable sufficient peak-shaving of the power grid within the DR period, while keeping the indoor temperature within an acceptable range. When the energy-storage tank could not meet the required response time, we used GTA to reduce the impact on user comfort. Using the thermal comfort level evaluation index, which was introduced in Section 2, we conducted a comparison between the two methods — see Table 7. Both the GTA method and the ACES+GTA method for a typical day, DAY2, when the actual temperature range for the indoor room was about level 0, the ratio of the time of the actual indoor temperature in [26, 26.5] to the total DR time of a day for the two operating modes are 16.7% and 55.8%, respectively. However, the percentages for level 3 were 66.7% and 25.8%. Clearly, the ACES+GTA method reduces the impact of temperature changes on thermal comfort (during the DR period) effectively.

(3) Economic analysis of the operation

When the temperature of the air-conditioning system was increased by 2 °C during the DR period for a typical day, Day2, the following results were calculated using Eqs. (1)–(3). The daily power consumption, load reduction, and subsidy costs, for the

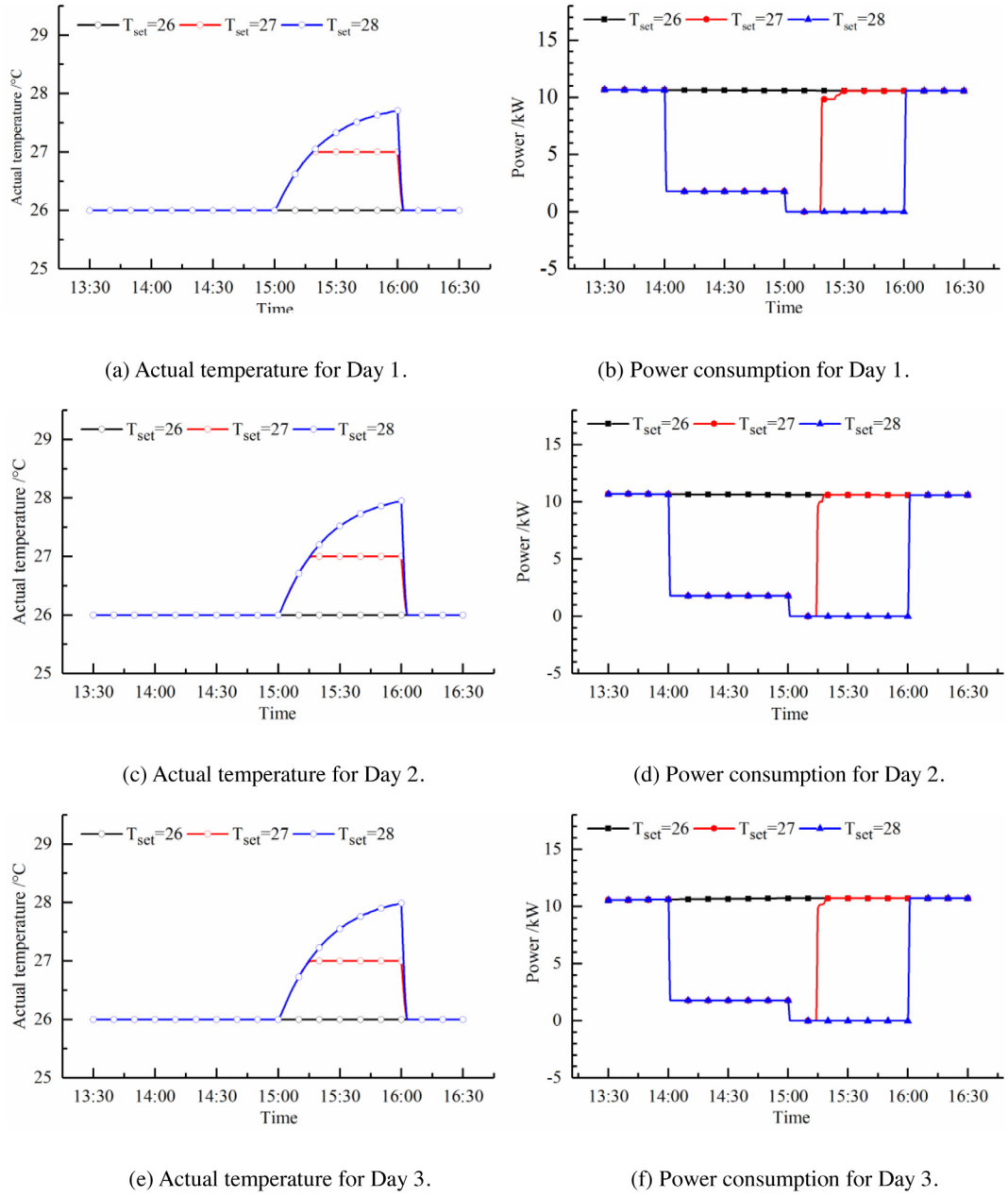

Fig. 14. ACES+GTA method: actual room temperature and corresponding air-conditioning system power-consumption changes.

Table 8
Comparison of daily power consumption, power-load reduction and subsidy costs for the two methods.

Policy	GTA	ACES+GTA
$W_{d.DR}$/kWh	82.0	84.8
$\alpha_{d.save}$/%	12.4	9.4
Power-load reduction/kWh	11.5	17.9
E_{DR}/$	35.2	55.7

Table 9
Comparison of the operating costs for the two methods and three different electricity prices.

Strategy	GTA			ACES+GTA		
Type of electricity price	TOU	RTP	CPP	TOU	RTP	CPP
$F_{d.DR}$/$	9.0	9.7	9.2	9.3	10.1	9.5
$C_{d.run}$/$	4.0	4.71	4.1	1.4	2.1	1.5
$F_{h.DR}$/$	0.9	0.9	1.0	0.4	0.4	0.5
$\alpha_{DR.save}$/%	60.6	55.2	62.9	81.9	82.7	82.1

GTA and ACES+GTA methods, are shown in Table 8. The operating costs for the two methods are shown in Table 9.

Using a comparative analysis for the two methods, it was not difficult to find that, even though the daily electricity consumption and operating cost($F_{d.DR}$) for the ACES+GTA method were higher than the GTA method, and the daily power-saving rate was lower than the GTA method, the cost for the ACES+GTA method (operating during the DR period) was lower than for the GTA method. In addition, its load reduction, subsidy fee, and DR time-saving rate were significantly better than for the GTA method. The daily costs, $C_{d.run}$, for GTA and ACES+GTA, for the TOU electricity-price curve, were 4.0 $ and 1.4 $, respectively.

For air-conditioning systems, the DR methods can only be implemented when the grid sends out a response signal. The number of responses was limited, and on most operating days

Table 10
Comparison of operating costs between energy storage and conventional (no energy-storage) operation methods.

Type	Power consumption/kWh	TOU/$	RTP/$	CPP/$
No energy-storage	5128.74	574.21	595.64	590.18
Energy storage	5147.15	534.97	564.49	550.94

conventional operating methods were used. When the DR was not considered, the electricity consumption for both the conventional (no energy storage) operation mode and the conventional operation mode, considering energy storage during the entire cooling season and the operating costs under different electricity prices, are shown in Table 10. Here, the conventional operation mode for energy storage was based on the system cost. The optimal cost target was to change the energy-release period for the energy storage water tank to the peak of the electricity price (between 10:00 and 15:00).

Table 10 shows that, compared to no energy-storage systems, even though the electricity consumption of the small-scale water storage system throughout the cooling season was slightly increased, its operating cost was relatively low. The conventional energy-storage operation mode, with the goal to optimize operating cost, had savings rates of 6.83%, 5.23%, and 6.65%, when using TOU, RTP, and CPP electricity-price schemes, respectively. However, because the optimal cost, which was described earlier in this paper, was based on the TOU electricity price, the rate of savings, using RTP and CPP, was not optimal. According to the three electricity price curves, when storing energy from 6:00 to 7:00, the electricity prices of TOU and CPP were low, and the RTP electricity price did fall into the lowest period. When the energy was released between 12:00–13:00, both TOU and RTP fell within the peak electricity price segment, and the CPP electricity price was not within the peak electricity price segment. Therefore, the optimal cost storage operation period was also different for different electricity price schemes. In addition, the operating-cost optimization needs to be adjusted, based on different electricity price models.

The total number of days, when the outdoor air-temperature exceeded 36 °C during the cooling season, was 13 days — of which 9 days fell within weekdays. Assuming that DR was implemented for the 9 days, the ACES+GTA method was used for the DR days, while for non-DR days the conventional operation method was used, which aims to optimize cost. Considering the TOU electricity price scheme for the calculation, the operating cost for the air-conditioning system was around 476 $. Furthermore, using the system operating cost indicator, F_{save}, see Eq. (4), we find that, compared with the case, where all days use conventional (no storage) operating modes, and considering the active energy-storage case, the HVAC system saved operating costs, F_{save}, of about 99 $. This represents a saving rate of 17.26%. Compared to the GTA method, which was used for the DR period, and the conventional (no storage) operating method, which was used during the non-DR period, the savings rate for the ACES+GTA method during the DR period (using active energy-storage during the non-DR period), was 7.02%.

4. Conclusions

We introduced and studied a HVAC DR method (ACES+GTA), which takes into account active energy-storage (based on the GTA method). Measurements with different daily DR operating methods were conducted, which verified the simulation. The experimental results showed that, when the energy-storage tank was used as a buffer component, the number of on/off switching of the ASHP could be effectively reduced for the actual operating modes (“high flow-rate, low cooling-load”). Moreover, it was found that the small-scale chilled-water storage system could effectively improve the flexibility of the building’s energy consumption and thereby help the air-conditioning system contribute to the DR. This result was confirmed by both measurements and simulation. When DR was used, the ACES+GTA method enabled a stable peak-clipping load and a stable clipping period for the power grid, which has a better response potential and response effect. In addition, compared to the ACES+GTA method, the peak-clipping potential of the GTA method could decrease with the increase of the room’s hourly cooling-load during the DR period. In this case, however, the peak-clipping load was unstable. Although the daily electricity consumption and operating cost of the ACES+GTA method were higher than for the GTA method, the ACES+GTA method showed lower daily operating costs for the air-conditioning system due to the subsidies during the DR period. For the ACES method, the impact of increasing the temperature setting on thermal comfort was relatively small. In addition, compared to the operation method without energy storage, a small-scale chilled-water storage system was able to save operating costs by 17.26% during the cooling season. At the same time, compared to GTA during the DR period and the conventional (no energy storage) operation method for the non-DR period, the saving rate (for the ACES+GTA method during the DR period and the energy storage used during the non-DR period), was 7.02%.

The ACES+GTA method considered the impact of the electricity price scheme on the operating cost of the HVAC system. It makes full use of the characteristics of the active energy-storage of the HVAC system. Furthermore, it provides auxiliary services for the DR for the power grid, without affecting the thermal comfort of the users. This method can affect the users’ electricity consumption behavior by reducing the operating cost of the HVAC system.

We only studied the operating cost of the air-conditioning system for three specific electricity-price schemes, based on the ACES+GTA method. Further studies would be beneficial to effectively regulate the air-conditioning system using different electricity-price schemes. In particular, dynamic electricity-prices, which change with the market in real-time, could reduce operating cost even more effectively. The ACES+GTA method should be tested in real buildings to verify the active energy-storage DR method proposed in this study.

CRediT authorship contribution statement

Qinglong Meng: Conceptualization, Methodology, Supervision, Funding acquisition. **Yang Li:** Software, Writing - original draft. **Xiaoxiao Ren:** Formal analysis, Data Curation. **Chengyan Xiong:** Data Curation, Writing - review & editing. **Wenqiang Wang:** Methodology, Writing - original draft. **Jiewei You:** Writing - review & editing.

Declaration of competing interest

The authors declare that they have no known competing financial interests or personal relationships that could have appeared to influence the work reported in this paper.

Acknowledgments

This work was supported by the Key Research and Development Program of Shaanxi, China (Grant No. 2020NY-204), the Fundamental Research Funds for the Central Universities, CHD, China (Grant No. 300102289103) and the Shandong Key Laboratory of Renewable Energy Technologies for Buildings, Jinan, 250101, China (Grant No. JDADS02).

References

Aghniaey, S., Lawrence, T.M., 2018. The impact of increased cooling setpoint temperature during demand response events on occupant thermal comfort in commercial buildings: A review. Energy Build. 173, 19–27. http://dx.doi.org/10.1016/j.enbuild.2018.04.068.

Amin, U., Hossain, M.J., Fernandez, E., 2020. Optimal price based control of HVAC systems in multizone office buildings for demand response. J. Clean. Prod. 270, 122059. http://dx.doi.org/10.1016/j.jclepro.2020.122059.

ASHRAE, 2013. ASHRAE Handbook-Fundamentals (SI). ASHRAE, Atlanta.

Beil, I., Hiskens, I.A., Backhaus, S., 2015. Round-trip efficiency of fast demand response in a large commercial air conditioner. Energy Build. 97, 47–55. http://dx.doi.org/10.1109/JPROC.2016.2520640.

Beil, I., Hiskens, I.A., Backhaus, S., 2016. Frequency regulation from commercial building HVAC demand response. Proc. IEEE 104 (4), 745–757. http://dx.doi.org/10.1016/j.enbuild.2015.03.028.

Candanedo, J.A., et al., 2015. Near-optimal transition between temperature setpoints for peak load reduction in small buildings. Energy Build. 87, 123–133. http://dx.doi.org/10.1016/j.enbuild.2014.11.021.

Chua, K.J., et al., 2013. Achieving better energy-efficient air conditioning – a review of technologies and strategies. Appl. Energy 104, 87–104. http://dx.doi.org/10.1016/j.apenergy.2012.10.037.

Cui, B., et al., 2015. Effectiveness and life-cycle cost–benefit analysis of active cold storages for building demand management for smart grid applications. Appl. Energy 147, 523–535. http://dx.doi.org/10.1016/j.apenergy.2015.03.041.

Cui, B., et al., 2017. Model-based optimal design of active cool thermal energy storage for maximal life-cycle cost saving from demand management in commercial buildings. Appl. Energy 201, 382–396. http://dx.doi.org/10.1016/j.apenergy.2016.12.035.

Dong, J., Xue, G., Li, R., 2016. Demand response in China: Regulations, pilot projects and recommendations - a review. Renew. Sustain. Energy Rev. 59, 13–27. http://dx.doi.org/10.1016/j.rser.2015.12.130.

Dongwen, C., et al., 2017. Planning, modeling and optimizing of cold-storage air-conditioning system for reducing peak load of industrial park. Electr. Power Autom. Equip. 36 (06), 94–100. http://dx.doi.org/10.16081/j.issn.1006-6047.2017.06.013.

Gupta, S.k., Ghose, T., Chatterjee, K., 2018. Droop based dynamic demand response controller for HVAC load. In: 2018 20th National Power Systems Conference (NPSC). Tiruchirappalli, India, http://dx.doi.org/10.1109/NPSC.2018.8771754.

Han, J., Piette, M.A., 2007. Solutions for summer electric power shortages: Demand response andits applications in air conditioning and refrigerating systems. Refrig. Air-Cond. 29 (1).

Hao, H., et al., 2017. Transactive control of commercial buildings for demand response. IEEE Trans. Power Syst. 32 (1), 774–783. http://dx.doi.org/10.1109/TPWRS.2016.2559485.

Jones, C.B., Carter, C., 2017. Trusted interconnections between a centralized controller and commercial building HVAC systems for reliable demand response. IEEE Access 5, 11063–11073. http://dx.doi.org/10.1109/ACCESS.2017.2714647.

Lam, T.N.T., et al., 2010. Impact of climate change on commercial sector air conditioning energy consumption in subtropical Hong Kong. Appl. Energy 87 (7), 2321–2327. http://dx.doi.org/10.1016/j.apenergy.2009.11.003.

Lee, T., et al., 2008. Optimization and implementation of a load control scheduler using relaxed dynamic programming for large air conditioner loads. IEEE Trans. Power Syst. 23 (2), 691–702. http://dx.doi.org/10.1109/tpwrs.2008.919311.

Li, W., et al., 2016. Electricity demand response in China: Status, feasible market schemes and pilots. Energy 114, 981–994. http://dx.doi.org/10.1016/j.energy.2016.08.081.

Liao, R., et al., 2012. Weather-clustering based strategy design for dynamic demand response building HVAC control. In: Proceedings of the Fourth ACM Workshop on Embedded Sensing Systems for Energy-Efficiency in Buildings. Association for Computing Machinery, New York, pp. 33–35. http://dx.doi.org/10.1145/2422531.2422537.

Lo, C.-C., Tsai, S.-H., Lin, B.-S., 2016. Ice storage air-conditioning system simulation with dynamic electricity pricing: A demand response study. Energies 9 (113), http://dx.doi.org/10.3390/en9020113.

Motegi, N., et al., 2007. Introduction to Commercial Building Control Strategies and Techniques for Demand Response - Appendices. Report No. LBNL-59975, http://dx.doi.org/10.2172/1004169, Retrieved from http://www.osti.gov/servlets/purl/1004169 (accessed 06 Augest 2019).

Moura, P.S., de Almeida, A.T., 2010. The role of demand-side management in the grid integration of wind power. Appl. Energy 87 (8), 2581–2588. http://dx.doi.org/10.1016/j.apenergy.2010.03.019.

Patteeuw, D., et al., 2015. Integrated modeling of active demand response with electric heating systems coupled to thermal energy storage systems. Appl. Energy 151, 306–319. http://dx.doi.org/10.1016/j.apenergy.2015.04.014.

Piette, M.A., et al., 2004. Development and Evaluation of Fully Automated Demand Response in Large Facilities. Report No. LBNL-55085, Retrieved from hittp://www.osti.gov/biblio/840331 (accessed 06 Augest 2019).

Piette, M., et al., 2005. Findings from the 2004 Fully Automated Demand Response Tests in Large Facilities. Report No. LBNL-58178, Lawrence Berkeley National Laboratory, Retrieved from hittp://www.smartgrid.gov/document/findings_2004_fully_automated_demand_response_tests_large_facilities (accessed 06 Augest 2019).

Pombeiro, H., Machado, M.J., Silva, C., 2017. Dynamic programming and genetic algorithms to control an HVAC system: Maximizing thermal comfort and minimizing cost with PV production and storage. Sustain. Cities Soc. 34, 228–238. http://dx.doi.org/10.1016/j.scs.2017.05.021.

Ran, F., et al., 2020. A virtual sensor based self-adjusting control for HVAC fast demand response in commercial buildings towards smart grid applications. Appl. Energy 269, 115103. http://dx.doi.org/10.1016/j.apenergy.2020.115103.

Rusa, W., 2015. Balancing Energy Efficiency and Cost-Effectiveness Evaluation System for Chiller Plant with Thermal Storage (Master). Tsinghua University.

Shen, W.M., Ma, Z.Q., Ma, J.J., 2019. The single peak shaving load in jiangsu province exceeds 4 million kilowatts. Available: http://www.cpnn.com.cn/zdyw/201908/t20190805_1146543.html (accessed 05 Augest 2019).

Wang, J., et al., 2010. Demand response in China. Energy 35 (4), 1592–1597. http://dx.doi.org/10.1016/j.rser.2015.12.130.

Wang, S., et al., 2016. Cooling supply-based HVAC system control for fast demand response of buildings to urgent requests of smart grids. Energy Procedia 103, 34–39. http://dx.doi.org/10.1016/j.egypro.2016.11.245.

Xiao-Jin, D.U., et al., 2006. Comparison on technical schemes of duty-cycling control in central air-conditioning system. Power Demand Side Manag. 8 (3), 31–32. http://dx.doi.org/10.3969/j.issn.1009-1831.2006.03.013.

Xin, J., Liang, W.U., 2013. Hierarchical strategies for duty cycling control of air conditioners in business buildings. Autom. Electr. Power Syst. 37 (5), 49–54. http://dx.doi.org/10.7500/AEPS201204161.

Xu, P.E., 2009. Case study of demand shifting with thermal mass in two large commercial buildings. ASHRAE Trans. 115, 586–598.

Yan, C.C., et al., 2015. A novel air-conditioning system for proactive power demand response to smart grid. Energy Convers. Manag. 102, 239–246. http://dx.doi.org/10.1016/j.enconman.2014.09.072.

Yang, C.J., 2017. Opportunities and barriers to demand response in China. Resour. Conserv. Recycl. 121, 51–55. http://dx.doi.org/10.1016/j.resconrec.2015.11.015.

Yao, L., Chang, W.C., Yen, R.L., 2005. An iterative deepening genetic algorithm for scheduling of direct load control. IEEE Trans. Power Syst. 20 (3), 1414–1421. http://dx.doi.org/10.1109/tpwrs.2005.852151.

Yin, R., et al., 2016. Quantifying flexibility of commercial and residential loads for demand response using setpoint changes. Appl. Energy 177, 149–164. http://dx.doi.org/10.1016/j.apenergy.2016.05.090.

Yun, K., et al., 2017. The performance analysis of automated demand response control strategies for air conditionings adopted in American commercial buildings. Power Demand Side Manag. 019 (001), 60–64. http://dx.doi.org/10.3969/j.issn.1009-1831.2017.01.016.

Zhang, T.W., et al., 2016. The commercial building air conditioning load control strategies and its comprehensive application in automated demand response system of the U.S.. Power Demand Side Manag. http://dx.doi.org/10.3969/j.issn.1009-1831.2016.06.015.